

Electronic Supplementary Information

In situ nanochemical imaging of label-free drugs: a case study of antimalarials in *Plasmodium falciparum*-infected erythrocytes

Faustine Dubar^a, Sylvain Bohic^{* b,c}, Christian Slomianny^d, Jean-Charles Morin^e, Patrick Thomas^e, Hadidjatou Kalamou^f, Yann Guérardel^g, Peter Cloetens^c, Jamal Khalife^f, Christophe Biot^{* g}

^aUniversité Lille Nord de France, Université Lille1, Unité de Catalyse et Chimie du Solide - UMR CNRS 8181, 59652 Villeneuve d'Ascq Cedex, France.

^bInserm, U836, équipe 6 « Rayonnement synchrotron et recherches médicales », Grenoble Institut des Neurosciences, 38054 Grenoble, France.

^cEuropean Synchrotron Radiation Facility, ESRF, BP220, Grenoble, France. Tel : +33-476882852; E-mail : bohic@esrf.fr

^dUniversité Lille1, Inserm U1003 - Laboratoire de Physiologie Cellulaire, Bâtiment SN3, 59655 Villeneuve d'Ascq Cédex, France.

^eIPL Santé, Environnement Durable, 1 rue du Professeur Calmette 59046 Lille Cedex, France.

^fCIIL, Inserm U 1019, UMR CNRS 8024 Université Lille Nord de France, Institut Pasteur de Lille, 1 rue du Pr Calmette, 59019 Lille Cedex, France.

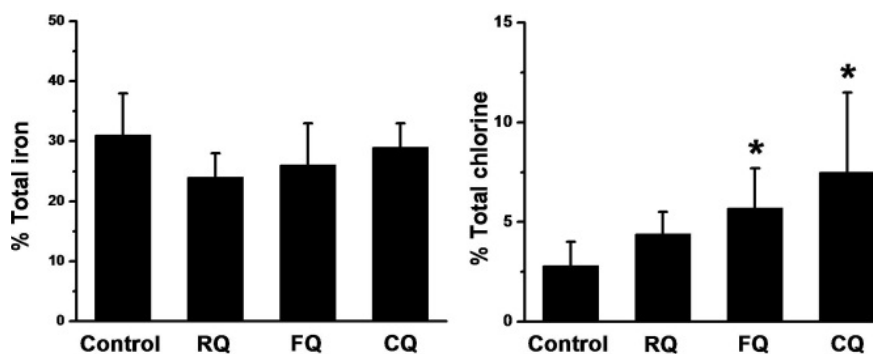
^gUniversité Lille Nord de France, Université Lille1, Unité de Glycobiologie Structurale et Fonctionnelle, CNRS UMR 8576, IFR 147, 59650 Villeneuve d'Ascq Cédex, France. Tel: +33-32043694 ; christophe.biot@univ-lille1.fr

Experimental Results

Table S1. ICP-MS determination of Ru concentration in uninfected and infected erythrocytes treated with RQ as a function of time.

t (min)	Ru uptake in infected erythrocytes (%)	Ru uptake in uninfected erythrocytes (%)	accumulation ratio
5	10.98	0.65	17
10	11.06	0.67	16
15	13.07	0.62	21
t (min)	RQ accumulation (%) in 1 μ L of media	RQ accumulation (%) in 1 μ L of infected erythrocytes	relative concentration in infected erythrocytes
5	0.06	10.99	184
10	0.06	11.07	187
15	0.06	13.07	215

Figure S1. Intra-erythrocytic distribution of the antimalarial drugs Ferroquine and Chloroquine in the HB3 strain of *P. falciparum* in vitro. Comparisons of the Fe and Cl concentrations in digestive vacuole and total iRBS permitted to evaluate the percentage of these elements within the digestive vacuole. Values are mean \pm S.D. (error bars), (*, $p < 0.05$).



Experimental Details

Methods

Chemicals. The compounds investigated in this study are presented in Figure 1. The synthesis of RQ has been previously reported by ourselves¹.

Cell culture. *Plasmodium falciparum* clones HB3 and W2 were routinely maintained in cultures in complete RPMI 1640 medium (25 mM HEPES and 300 mg/l l-glutamine; Invitrogen), enriched with 10% decompartmented human serum (AB+), and 6% human red blood cells (O+) at 37°C under controlled atmosphere (O₂ 5%/CO₂ 5%/N₂ 90%; Air Liquide, Paris, France). Serum and red blood cells were supplied by Centre Régional de Transfusion Sanguine, Lille, France. Cultures were controlled by thin smears stained with Giemsa (Merck, Darmstadt, Germany). Parasitemia were monitored on 1000 red blood cells.

The assays were carried out on synchronous *P. falciparum* cultures with ~10 parasitemia containing old trophozoites and 3% hematocrit. Ferroquine and ruthenoquine were added at a final concentration of 40 nM. After 30 min of incubation, the treated and untreated (DMSO alone) were fixed in a buffer containing 2.5% glutaraldehyde and 0.1 M sodium cacodylate.

ICP-MS Studies. Uninfected and *Plasmodium falciparum* HB3 strain infected RBC were digested with AAS conc. HNO₃ (65%) overnight (500 µL). 100 µL of hydrogen peroxide were added and the volume is fixed to 5 mL by addition of water.

The media were digested with AAS conc. HNO₃ (65%) overnight (1 mL). 200 µL of hydrogen peroxide were added and the volume is fixed to 5 mL by addition of water.

Samples were analyzed for Ru at "IPL santé, environnement durables" (Institut Pasteur de Lille, France) on a Thermofisher Scientific XSeries II Inductively Coupled Plasma Emission Mass Spectrometer (ICP-MS).

Synchrotron X-ray Fluorescence (XRF) Studies. Uninfected and *Plasmodium falciparum* HB3 strain infected RBC were deposited on 500-nm thick silicon nitride windows (Silson Pty Ltd), fixed in methanol and washed with distilled water. Normal RBC morphology was retained throughout the treatment and fixation procedures as evidenced in the optical micrographs.

Synchrotron X-ray fluorescence experiments were carried out at the nanoimaging end-station ID22NI of the European Synchrotron Radiation Facility (ESRF; Grenoble, France). Dynamically bent graded multilayers set in the Kirkpatrick–Baez geometry were used to focus the x-ray beam from an undulator source to a spot size of approximately 80 nm² on the sample. Regions of interest were chosen using an online optical microscope, which also allowed control of the beam position onto the sample. The sample, mounted in air at room temperature on a nanopositioner stage, was raster scanned with a step size of 100 nm through the focal plane, while the spectrum of the emitted fluorescence was recorded with an energy dispersive silicon drift diode collimated detector (SII Nanotechnology Vortex, 50 mm² sensitive area) placed in the horizontal plane at 75° from the incident beam². The integration time per scan point was 1s and normalization against variations in the synchrotron incident

beam intensity was achieved using a downstream Si PIN-diode detector. Five cell images were obtained for each of the conditions described. This allowed the generation of a pixel-by-pixel spectral image providing topographical elemental maps by fitting the full fluorescence spectrum at every single point using the PyMCA software³. Quantification was performed using fundamental parameter method revised and expanded implemented within the PyMCA software. NIST standards reference materials SRM1832 (thin film standard) and SRM1577b (bovine liver) were used to calibrate experimental parameters.

Despite 29 keV X-ray incident photons which are not absorbed by the cells, the number of incident photons is extremely high and some radiation damages occur burning the cells. Nevertheless, the cell exhibits the same shape at the same position before and after the analysis, as established by the high-resolution online video microscope on the nanoprobe. The samples were mounted on Si₃N₄ substrates that are not affected by the intense beam and we did not observe sample movements or shrinkage. This may happen when any types of cells are deposited on some thin polymer films backing that deform under rastering of the intense X-ray nanobeam.

About Fig. 2. The importance of the high spatial resolution of the technique and of the spectral fitting at each pixel of the elemental maps is here highlighted. Indeed, if we were limited by summing all spectrum at each pixel over the whole cell area, the Ru signal was drown in the background.

Intensity scale (reverse greyscale), the maximal value (mass fraction) is indicated for each elemental map:

Fig. 2a	Fe, 9.10^{-3}	Ru, 26.10^{-6}	Cl, 17.10^{-3}	S 5.10^{-3}
Fig. 2b	Fe, 6.10^{-3}		Cl, 8.10^{-3}	S 3.10^{-3}

About Fig. 3. Intensity scale (reverse greyscale), the maximal value (mass fraction) is indicated for each elemental map:

Control	Fe, $7.6.10^{-3}$	Cl, 10.0^{-3}	S, $3.2.10^{-3}$
CQ:	Fe, 14.10^{-3}	Cl, 28.10^{-3} ,	S, $3.5.10^{-3}$
FQ:	Fe, 11.10^{-3}	Cl, 12.10^{-3}	S, $2.3.10^{-3}$

Transmission electron microscopy. Cells were fixed with 2.5% glutaraldehyde in 0.1M cacodylate buffer (pH 7.2) for 1 h at 4°C, followed by 1% OsO₄ for 30 min at 4°C. Subsequently, cells were dehydrated through a graded series of acetonitrile and embedded in epoxy resin. Thin sections (100 nm) were cut on a Reichert Ultracut E ultramicrotome, placed

on 100-mesh copper grids and viewed under a Hitachi H600 electron microscope (Tokyo, Japan) at 75kV acceleration voltage. The spatial resolution was 2 nm.

Acknowledgment. We acknowledge the European Synchrotron Radiation Facility for provision of synchrotron radiation facilities. The authors thank Philippe Vervaecke for critical reading of the manuscript. This study was funded by a grant from the Minis-tère de l'Enseignement Supérieur to F.D..

1. F. Dubar, T. J. Egan, B. Pradines, D. Kuter, K. K. Ncokazi, D. Forge, J.-F. Paul, C. Pierrot, H. Kalamou, J. Khalife, E. Buisine, C. Rogier, H. Vezin, I. Forfar, C. Slomianny, X. Trivelli, S. Kapishnikov, L. Leiserowitz, D. Dive, et C. Biot, *ACS Chem. Biol.*, 2011, **6**, 275-287.
2. D. J. Lewis, C. Bruce, S. Bohic, P. Cloetens, S. P. Hammond, D. Arbon, S. Blair-Reid, Z. Pikramenou, et B. Kysela, *Nanomedicine (Lond)*, 2010, **5**, 1547-1557.
3. V. A. Solé, E. Papillon, M. Cotte, P. Walter, et J. Susini, *Spectrochimica Acta Part B: Atomic Spectroscopy*, 2007, **62**, 63-68.